14th IEA Heat Pump Conference
15-18 May 2023, Chicago, Illinois

Decarbonizing Steam Generation with High Temperature Heat Pumps: Refrigerant Selection and Flowsheet Evaluation

Christoph Höges[a, *], Valerius Venzik[a], Christian Vering[a], Dirk Müller[a]

[a] Institute for Energy Efficient Buildings and Indoor Climate, Mathieustr. 10, 52074 Aachen, Germany

Abstract

High temperature heat pumps have a high potential to reduce carbon emissions in industrial processes by replacing conventional heating systems for low-pressure steam generation. However, heat pump performance is sensitive to the selected refrigerant, flow sheet, and operating conditions complicating the design process. Thus, we conduct a refrigerant selection and evaluate five flow sheets for a low-pressure steam application, which heats liquid water from 80°C at 1.5 bar to 120°C steam. First, refrigerants are screened to identify suitable low-GWP (<150) refrigerants. We find 15 alternative refrigerants. Second, the performance of the selected refrigerants is evaluated in five flow sheets, including two vapor injection and a parallel-compression configurations. R717 outperforms all other solutions concerning cycle efficiency and heating capacity for all investigated cycles. However, R717 leads to high compressor discharge temperatures limiting the applicability with compressor lubricant. Here, lubricant-free technologies such as turbo compressors are promising. Besides R717, the investigation shows further solutions with high efficiencies. Most promising refrigerants, however, have a double bond in their molecule structure, reducing their chemical stability. Furthermore, the cycle configuration using vapor injection in combination with an internal heat exchanger yields the highest cycle efficiencies. Compared to the simple flow sheet, more than 20% of improvements are possible.

Selection and/or peer-review under the responsibility of the organizers of the 14th IEA Heat Pump Conference 2023.

Keywords: hydrocarbons ; loss-based compressor model ; low-pressure steam ; R717

1. Introduction

To achieve the goals of the Paris Climate Agreement, carbon emissions have to be reduced. One main source of carbon emissions is the combustion of fossil fuels in heat generation with conventional systems, e.g., a gas boiler [1]. Heat pumps are a possible solution to replace conventional systems in heat generation. Heat pumps use ambient or waste heat combined with electric power to provide the necessary heat demand. Thereby, the emissions of the heat pump depend on the specific emissions of the necessary power demand and the emissions related to refrigerant leakages on-site.

In industrial processes, heat over a wide range of temperatures is needed to satisfy all demands [2]. A large share of the necessary heat is utilized at temperatures below 200 °C, which current heat pumps can provide. Thus, a considerable reduction of carbon emissions is possible that be utilized with heat pumps [3].

For many industrial processes (e.g., drying, refining, and food processing), steam is used to distribute the heat due to its high heat capacity and good transfer properties. In addition, due to its high latent heat, a large amount of heat can be provided while keeping the temperature constant. However, the literature on steam generation using a heat pump is limited. Furthermore, steam generation is especially challenging due to the high isothermal heat demand, which leads to a more complex secondary temperature curve in the condenser.

In contrast to conventional heating systems, heat pump efficiency strongly depends on the operating point. Additionally, the selected refrigerant and cycle configuration influence operational performance, leading to lower efficiency or a reduced operating range. For refrigerants, current regulations regarding a low global

* Corresponding author. Tel.: +49 241 80 49598; fax: +49 241 80 49769.
E-mail address: christoph.hoeges@eonerc.rwth-aachen.de.

warming potential (GWP) and a zero ozone depletion potential (ODP) should be met [4]. Additionally, the refrigerant is subject to thermodynamic requirements regarding the critical temperature, the isobaric heat capacity, and the latent heat to achieve high efficiencies. Furthermore, the molecule has to offer long-term chemical stability to ensure a safe and efficient operation. Thus, the number of potential refrigerants is limited on the one hand, and the identification is more complex compared to the residential heat pumps on the other hand.

Besides the refrigerant [5, 6], the cycle configuration, i.e., the selected components [7, 8] and flowsheet [9, 10], has a significant influence on the overall cycle performance and the operating envelope. In contrast to residential heat pumps that are well known, industry heat pumps have a much higher heating capacity, which can exceed several Megawatts. Furthermore, due to the high energy flows, the overall share of the operation period is significantly higher than conventional, small-scale heat pumps. Thus, improving the efficiency as much as possible is one key aspect when designing large-scale heat pumps, resulting in a broader number of possible cycle configurations.

In this work, we investigate the potential of heat pumps to generate steam at 1.5 bar pressure and analyze the influence of the refrigerant and the selected flowsheet on the overall cycle performance. First, a refrigerant selection based on thermodynamic and ecologic properties is conducted for the defined application. The selection leads to 14 refrigerants that are not toxic and have GWP below 150. Additionally, ammonia (R717) and R245fa are included due to their wide usage. Furthermore, we include a zeotropic mixture based on R600a and R601a to analyze the potential of zeotropic mixtures for the defined application. Second, a case study is conducted that heats liquid water from 80 °C to steam at 120 °C. The investigation uses five cycle configurations to analyze their influence on the optimal refrigerant. Third, the present study's findings are discussed, and future research aspects are mentioned that should be directed in the future.

2. Methodology

The following sections present the used cycle models and the use case parameter. First, the general evaluation procedure is presented. Afterward, the component modeling followed by the investigated cycles is shown. Finally, section 2.4 presents the parameters of the case study and the selected refrigeration of the investigation.

2.1. Modeling approach

We use consistent thermodynamic models to predict the heat pump cycle behavior. The expansion valve is isenthalpic. Piping and all further components have no pressure and heat losses. For modeling the heat exchangers, a pinch model is used, enabling to determine the evaporation and condensation pressures related to the heat source and sink. Fig. 1 shows the temperature curves of the heat source (blue) and heat sink (red). The heat source uses sensible heat with a constant heat capacity resulting in a linear curve. The heat sink is split into a sensible part (preheating liquid water), a latent part (evaporation of water), and a sensible part (superheating of water).

Further degrees of freedom of the process are the superheating ΔT_{SH} at the compressor inlet and the subcooling ΔT_{SC} at the condenser outlet.

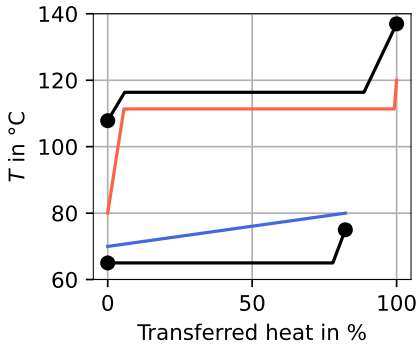

Fig. 1: Temperature curves of sink water (red) with cyclobutene (black) as the refrigerant and a heat source (blue).

As the main deviation from the standard heat pump model, the compressor efficiencies are calculated through a loss-based model of a reciprocating compressor [11]. The model calculates the isentropic and volumetric compressor efficiencies as a function of the operating point and the refrigerant. Equation (1) shows the general definition of the isentropic compressor efficiency η.

$$\eta = \frac{\dot{m}_{\text{refrigerant}} \cdot \Delta h_{\text{com}}^{\text{rev}}}{P_{\text{el}}} \tag{1}$$

The model includes multiple loss mechanisms within a compressor and combines them with analytical definitions of compressor efficiencies. Thereby, friction (parameter *a*), flow losses (parameter *b*), and electrical (parameter *c*) losses are considered. The model leads to the following expression for the isentropic compressor efficiency:

$$\eta = \frac{V_{\text{cyl}} \cdot n_{\text{cyl}} \cdot f_{\text{mech}} \cdot \rho_{\text{in}} \cdot \eta_{\text{vol}} \cdot \left(h_{\text{out}}^{\text{is}} - h_{\text{in}}\right)}{V_{\text{cyl}} \cdot n_{\text{cyl}} \cdot f_{\text{mech}} \cdot \rho_{\text{in}} \cdot \eta_{\text{vol}} \cdot \left(h_{\text{out}}^{\text{is}} - h_{\text{in}}\right) + a + b \cdot \rho_{\text{in}} \cdot (V_{\text{cyl}} \cdot n_{\text{cyl}} \cdot f_{\text{mech}} \cdot \eta_{\text{vol}})^3} (1 - c) \tag{2}$$

The volumetric compressor efficiency η_{vol} is approximated as a function of the pressure and refrigerant properties

$$\eta_{\text{vol}} = 1 - \frac{k_1}{H_{\text{ref}}} \cdot \left(\frac{p_{\text{out}} + k_2 \cdot \rho_{\text{in}}}{p_{\text{in}}}\right)^{\frac{c_{\text{v}}}{c_{\text{p}}}} \tag{3}$$

with k_1 and k_2 being fitting variables. Additionally, Roskosch et al. [11] proposed an approach that scales the loss parameters of friction (*a*) and flow losses (*b*) by the compressor geometry (piston diameter *D* and stroke *H*). We will use this scaling approach in our study to design the compressor geometry specifically for each refrigerant concerning the desired heating power of the heat pump.

For the cycle calculation, we use an optimization approach. As a result, each investigated flowsheet's coefficient of performance (COP) is maximized. Equation (4) states the optimization problem based on boundary conditions $\vec{\theta}$.

$$\begin{aligned} &\max_{\vec{x}} COP\left(\vec{x}, \vec{\theta}\right) \\ s.t. \quad &g\left(\vec{x}, \vec{\theta}\right) \geq 0 \\ &\vec{x}_{\min} \leq \vec{x} \leq \vec{x}_{\max} \end{aligned} \tag{4}$$

The optimizer permutes the optimization variables of vector $\vec{x}$, which depend on the flow sheet (see section 2.2). To speed up the calculation, reasonable lower and upper limits $\vec{x}_{\min}$ and $\vec{x}_{\max}$ are defined, respectively. Additionally, the cycle calculation is subject to multiple inequality constraints $g\left(\vec{x}, \vec{\theta}\right)$ that ensure a physical operation.

The inequality constraints *g* ensure a physically and technically feasible operation and include three main constraints. The first constraint prevents supercritical operation [12]. The second constraint verifies that no wet compression occurs, i.e., liquid droplets during compression [13]. The compression is discretized in thirty steps, and the respective specific enthalpy is compared to the dew line enthalpy. The third constraint is part of the pinch model and ensures that a minimum approach temperature within all heat exchangers (condenser, evaporator, internal heat exchanger) is kept.

2.2. Investigated flowsheets

The present work investigates five flowsheets. Fig. 2 shows their schematics. In the following subsections, their general modeling assumptions are presented A detailed description can be found in [14]. To calculate the individual fluid properties, the *REFPROP* fluid database [15] is used.

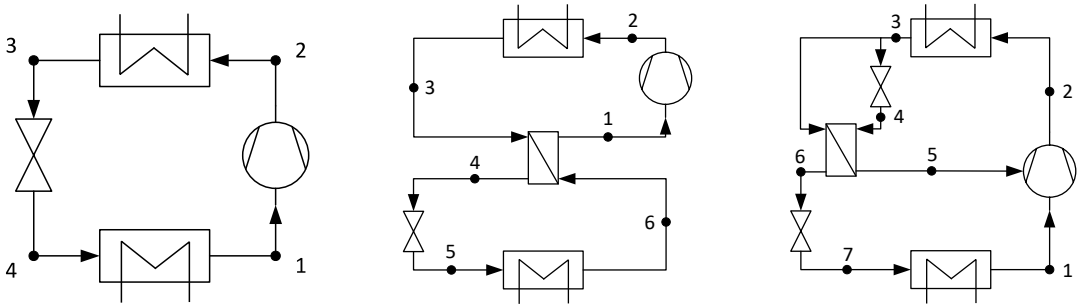

(a) simple (b) ihx (c) vi

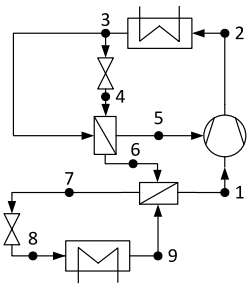

(d) vi-ihx

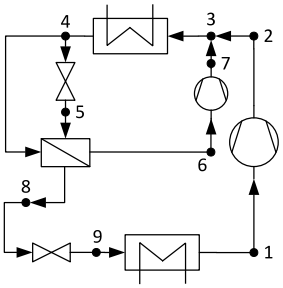

(e) pc

Fig. 2: Investigated flowsheets for steam generation heat pumps.

2.2.1. Simple cycle (Fig. 2a)

The cycle simulation of the simple cycle uses four degrees of freedom, which are defined by equation (5).

$$\vec{x}_{\text{simple}} = [p_{\text{eva}};\ p_{\text{con}};\ \Delta T_{\text{SH}};\ \Delta T_{\text{SC}}]^T \tag{5}$$

Here, the evaporation pressure p_{eva}, the condensation pressure p_{con}, the superheating ΔT_{SH} at the compressor inlet, and the subcooling ΔT_{SC} at the condenser outlet need to be defined. As the main assessment criterion, the *COP* is the ratio of transferred heat within the condenser and the electric power demand in the compressor. Equation (6) shows the formulation for the simple cycle assessment.

$$COP_{\text{simple}} = \frac{\dot{Q}_{\text{con}}}{P_{\text{el}}} = \frac{h_2 - h_3}{h_2 - h_1} \tag{6}$$

2.2.2. Internal heat exchanger cycle (Fig. 2b)

For the internal heat exchanger, we assume that a heat transfer from the condenser outlet realizes the entire superheating at the compressor inlet. Therefore, the refrigerant leaves the evaporator as saturated vapor and the condenser already as a subcooled liquid while it is superheated and further subcooled in the internal heat exchanger. Overall, the degrees of freedom, as well as the target function *COP*, are the same compared to the simple cycle (c.f. equation (5) and (6)). Here, we assume that the internal heat exchanger is designed ideally for the application. Thus, we optimize the transferred heat and do not use an efficiency based modeling approach.

2.2.3. Vapor injection cycle (Fig. 2c)

For the vapor injection (vi), a two-stage compression is used. After the first stage, the condenser outlet is split, and a partial mass flow rate $\dot{m}_{\text{inj}}$ (state 5) is injected into the compressor. Due to the vapor injection, the cycle includes additional degrees of freedom. Thus, the intermediate pressure p_{int} of states 4 and 5 is optimized. The injection ratio *y*, which is the ratio of injected vapor $\dot{m}_{\text{inj}}$ and total mass flow rate in the condenser $\dot{m}_{\text{con}}$, is included.

$$y = \frac{\dot{m}_{\text{inj}}}{\dot{m}_{\text{con}}} \tag{7}$$

$$\vec{x}_{\text{vi}} = [p_{\text{eva}};\ p_{\text{con}};\ \Delta T_{\text{SH}};\ \Delta T_{\text{SC}};\ p_{\text{int}};\ y]^T \tag{8}$$

The injected mass flow rate is at state 5 always saturated vapor. Due to the two-step compression and vapor injection into the compression chamber, the cycle efficiency calculation is more complex than the simple heat pump cycle. Equation (9) shows the definition of the *COP* for the vi cycle.

$$COP_{\text{vi}} = \frac{h_2 - h_3}{(1-y)\cdot \Delta h_{\text{com,step},1} + \Delta h_{\text{com,step},2}} \tag{9}$$

Thereby, $\Delta h_{\text{com,step } i}$ is the specific enthalpy difference due to the compression in step *i*. Since the mass flow within the evaporator and thus, the first compression step only includes a partial mass flow rate.

2.2.4. Vapor injection in combination with the internal heat exchanger cycle (Fig. 2d)

The fourth cycle combines the advantages of the internal heat exchanger cycle (cf. section 2.2.2) and the vapor injection cycle (cf. section 2.2.3). Degrees of freedom, and the COP calculation, are similar to the vapor injection cycle (cf. equation (8) and (9)).

2.2.5. Parallel compression cycle (Fig. 2e)

The parallel compression cycle (pc) functionality is similar to the vapor injection cycle. However, instead of a two-stage compression process with injection in a single compressor, the flowsheet includes two individual compressors. In parallel compression, the split and preheated mass flow rate (state 6) is not injected into the main compressor but compressed by a second compressor (state 7). Here, state 6 needs the minimum amount of superheating to ensure the compressor's safe operation. Afterward, compressor outlets are mixed (state 3) and enter the condenser. Overall, the degrees of freedom is similar to the vapor injection cycle (cf. section 2.2.3). However, the calculation of the *COP* deviates:

$$COP_{\mathrm{pc}} = \frac{h_2 - h_3}{y \cdot \Delta h_{\mathrm{com},67} + \Delta h_{\mathrm{com},12}} \tag{10}$$

2.3. Case study

The present investigation aims to cover the following research questions:

1. Which refrigerants show high efficiency and are suitable for a steam generation?
2. Which flowsheet shows the overall best performance?
3. How do the results regarding the optimal flowsheet deviate for different refrigerants?
4. How does the source temperature influence the overall results?

To do so, the investigation focuses on steam generation where liquid water enters the condenser at 80 °C and 1.5 bar and leaves the condenser as superheated vapor at 120 °C and 1.5 bar. Five different inlet temperatures are investigated for the heat source, ranging from 40 to 80 °C. For each temperature, the temperature difference of the source is set to 10 K. Fig. 1 shows the temperature curves in both heat exchangers for the sink, source, and refrigerant.

For the defined application, a fluid selection is conducted. The fluid selection accounts for global warming potential (GWP) limits and the minimum operating pressure at an evaporation temperature of 30 °C. Additionally, the filter only includes non-toxic fluids and limits the operation to subcritical. Thus, refrigerants with a critical temperature below 130 °C are dropped. As a result, 14 refrigerants satisfy the defined constraints. For some selected refrigerants, though, the actual GWP value is low. Since all of them are isomeres of known hydrocarbons, their expected GWP value should be below 150. Therefore, in addition to the selected refrigerants, ammonia and R245fa are added: Ammonia due to its high performance in the literature and R245fa as a reference refrigerant. Lastly, a zeotropic mixture based on R600a and R601a with a molar composition of 75/25 is included to analyze the potential of zeotropic mixtures for steam generation. Table 1 shows the selected refrigerants and their properties.

Table 1: Fluid properties of preselected pure refrigerants. Some fluid properties are not given in the literature, and their value is set to not available (n.a.).

Refrigerant	Molar mass [g/mol]	T_{crit} [°C]	NBP [°C]	ODP	GWP	Safety class	Molecule: Double or triple bind?
R601a (isopentane)	72.2	187.2	27.5	0	5	A3	no
R600a (isobutane)	58.1	134.6	-11.7	0	3	A3	no
R600 (butane)	58.1	152.0	-0.5	0	4	A3	no
R717 (ammonia)	17.0	132.4	-33.6	0	0	B2L	no
R1224yd(Z)	148.5	155.3	14.3	0.00012	< 1	A1	yes
R1233zd(E)	130.5	166.5	17.9	0.00034	1	A1	yes
R1234ze(Z)	114.0	150.1	9.4	0	1	A1	yes
R1336mzz(Z)	164.1	171.4	33.1	0	2	A1	yes
R1336mzz(E)	164.1	130.4	7.6	0	18	A1	yes
Butene	56.1	146.1	-6.6	0	n.a.	A3	yes
Isobutene	56.1	144.9	-7.3	0	n.a.	A3	yes
Cyclobutene	54.1	174.9	2.2	0	n.a.	A3	yes
1-Butyne	54.1	158.9	7.7	0	n.a.	A3	yes (3)
(Z)-But-2-ene	56.1	162.6	3.4	0	n.a.	A3	yes
(E)-But-2-ene	56.1	155.5	0.5	0	n.a.	A3	yes
R245fa	134.1	153.9	14.7	0	858	B1	no

Besides the parameters of the overall case study, the models presented in section 2.2 need lower and upper bounds for the defined degrees of freedom. The lower and upper bound should be set as close as possible to reduce the overall optimization time while not influencing the overall investigation results. Table 2 shows the selected bounds of the case study.

Table 2: The flowsheet evaluation's lower and upper bounds of optimization parameters.

Optimization parameters	Lower bound	Upper bound
Evaporation pressure p_{eva}	p_{dew}@283.15 K	$p_{\mathrm{dew}}@T_{\mathrm{eva,sec,in}}$
Condensation pressure p_{con}	$p_{\mathrm{dew}}@T_{\mathrm{con,sec,in}}$	$p_{\mathrm{dew}}@(T_{\mathrm{con,sec,out}} + 20$ K)
Amount of superheating ΔT_{SH} in K	10	30
Amount of subcooling ΔT_{SC} in K	0	40
Intermediate pressure ratio *r*	0	1
Injection ratio *y*	0	0.5

3. Results

The following section presents the results of the conducted investigation. The study includes all refrigerants mentioned in Table 1. However, the figures in this work show only a selected number of refrigerants that represent the overall findings. Table 3 in the attachment shows the complete results for all mentioned cycle configurations and refrigerants for the operating point W80/W120.

Fig. 3 shows the results for the *COP* for a sink and source inlet temperature of 80 °C. Starting with the simple cycle (red bars), ammonia (R717) shows the highest efficiency at 5.75, and R1336mzz(E) shows the lowest efficiency at 3.41. Besides ammonia, cyclobutane shows similar high efficiencies. However, all other refrigerants lead to significantly lower efficiencies.

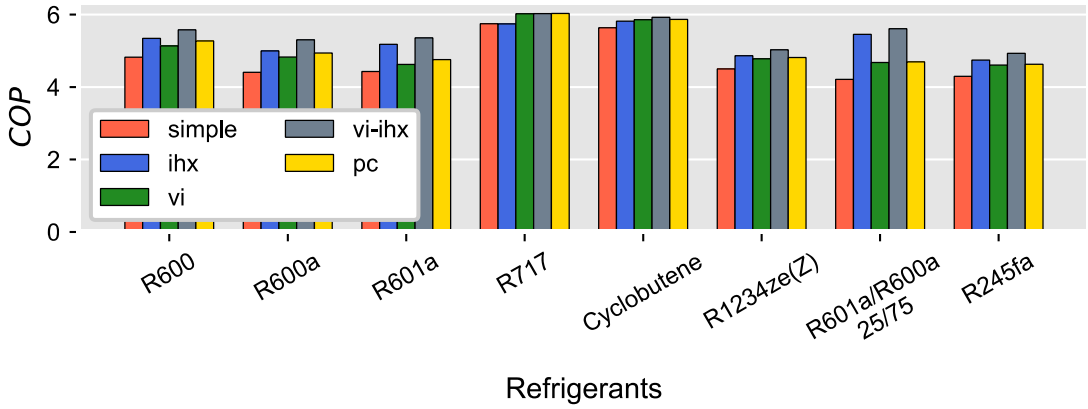

Fig. 3: *COP* of selected refrigerants with a sink and source inlet temperature of 80 °C.

Using the advanced flowsheets, ammonia and cyclobutane still lead to the highest efficiencies. The highest efficiency of 6.03 (R717) is reached when the vapor injection cycle, in combination with an internal heat exchanger, is used, leading to improvements of approximately 5 %. For both refrigerants, the improvements are relatively small compared to the other refrigerants. In contrast to both high-performance refrigerants, the efficiency of the zeotropic mixture based on R601a and R600a depends much more on the selected flowsheet. Here, the efficiency improves by up to 33 % with the advanced flowsheet vi-ihx. Thus, one observation is the strong interdependency of the refrigerant and the selected flowsheet.

The vi-ihx flowsheet leads to the highest overall efficiencies for all studied refrigerants, combining the ihx and the vi flowsheet. Additionally, the ihx flowsheet shows the second-highest efficiencies except for ammonia and cyclobutene. In the ihx flowsheet, the amount of superheating is shifted from the evaporator into the internal heat exchanger. Consequently, two effects occur for a perfect counterflow evaporator, which is assumed in the present work. First, the pinch-point shifts from the refrigerant outlet to the refrigerant inlet for a pure refrigerant. As a result, the lower pressure level increases, resulting in lower pressure ratios and, thus, higher efficiencies. Second, the heat that can be utilized in the evaporator increases due to the heat recovery

rate and the resulting lower vapor quality at the evaporator inlet. The heat recovery rate results from the higher superheating of the ihx cycle. Hence, the share of the provided heat received by the heat source increases, leading to higher efficiencies. However, one negative aspect is the increased maximum process temperatures (compressor discharge temperatures) due to the higher inlet temperatures in the compressor.

Fig. 4 shows the maximum process temperatures. Regarding the differences between the selected flowsheets, the ihx cycle shows the highest outlet temperatures for all refrigerants, followed by the vi-ihx cycle (except for ammonia). Due to the higher temperatures, the operating envelope of the compressor can be reduced. Thus, the overall operating range must be checked when selecting the compressor in combination with the flowsheet. On the other hand, the vi cycle leads to the lowest maximum temperatures. For the refrigerants, ammonia shows the highest process temperatures for all cycles, exceeding values above 160 °C.

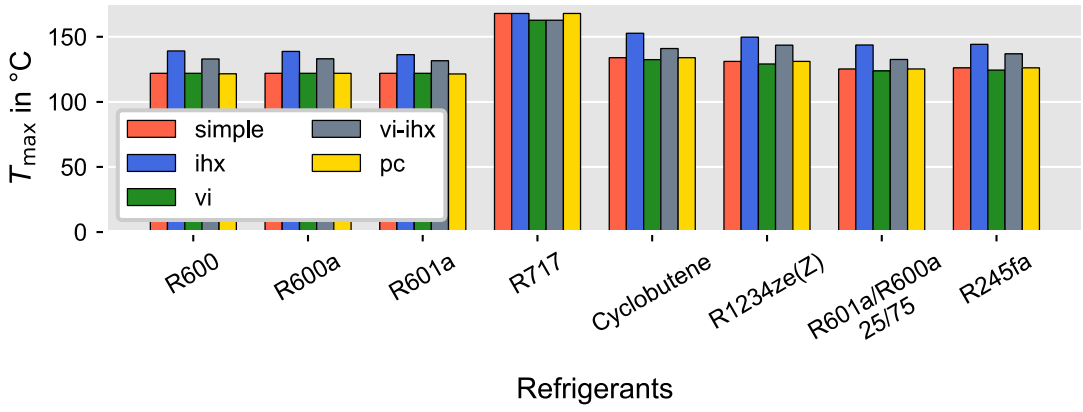

Fig. 4: Maximum process temperature for selected refrigerants in all cycle configurations for a source inlet temperature of 80 °C.

Besides the mentioned effects in the ihx cycle, the vi-ihx cycle adds the advantages of vapor injection to the ihx cycle, resulting in even higher efficiencies. When using vapor injection, the compressor outlet temperature decreases due to the injection of steam at a lower temperature. The lower compressor outlet and, thus, condenser inlet temperature leads to a lower mean temperature difference between the refrigerant and the secondary fluid (in this case, water) in the condenser, reducing the entropy production during the heat transfer and, thus, leading to higher efficiencies. Additionally, the throttling losses are reduced since only a partial mass flow rate is expanded to the evaporation pressure, whereas the other part only expands to the intermediate pressure. Thus, the overall losses can be reduced.

However, the amount of loss reduction when changing the flowsheet depends on the refrigerant. Thus, not all refrigerants show the same results. In this case, the most significant improvement when changing the flowsheet occurs for the zeotropic mixture. Here, up to 33 % improvements are presented when changing the flowsheets from the simple to the vi-ihx cycle. The main reason is the even higher effect of the internal heat exchanger for zeotropic mixtures. For pure fluids, the pinch point in the evaporator is located at the evaporator inlet in case no superheating is provided in the evaporator. For zeotropic mixtures with a temperature glide that perfectly matches the source temperature difference, however, the pinch-point can still be located at the evaporator outlet. Thus, the evaporation pressure can rise even further when using an internal heat exchanger, leading to higher efficiency improvements.

Nevertheless, the zeotropic mixtures still show far lower efficiencies than high-performing refrigerants like ammonia. The main reason here is the mainly latent temperature curve of the sink water in the condenser. In the condenser, the temperature glide can not be utilized due to the mainly isothermal heat transfer to the sink water. Therefore, the mean temperature difference between refrigerant and water increases if the refrigerant has a temperature glide. Once the mean temperature difference increases, the losses due to heat transfer also increase, resulting in lower overall efficiencies. Thus, zeotropic mixtures are not suitable for the generation of steam. However, azeotropic mixtures with similar behavior to pure fluids could increase efficiency since their overall fluid properties can be tailor-made by adjusting the mixture composition. Thus, azeotropic mixtures should be investigated further for applying steam generation heat pumps.

When comparing the pure refrigerants given in Fig. 3, most refrigerants show similar behavior when adjusting the flowsheet. Ammonia, however, deviates from the general performance adjustments. To analyze the effects further, Fig. 5 compares the results for all flowsheets for five source temperatures for the refrigerants ammonia (R717 – left) and butane (R600 – right). For both refrigerants, all flowsheets show the highest

efficiencies for the highest source temperature, which is the fundamental phenomenon related to the Carnot principle. The performance of the individual flowsheets, however, changes significantly. The pc, vi, and vi-ihx cycles for ammonia show similar efficiencies for all operating points.

Additionally, the ihx and simple cycle show similar performances but lower than the other three flowsheets. For butane, the vi-ihx cycle leads to the highest efficiency for all source temperatures, followed by the ihx, vi, and pc. However, the performance ranking of the ihx, vi, and pc flowsheets depends on the operating point. For high source temperatures (lower temperature lifts), the ihx flowsheet is superior to the other two. With decreasing source temperature and, thus, increasing temperature lift, the vi and pc flowsheet's potential increases, outperforming the ihx cycle's potential. Once again, the simple cycle shows the lowest efficiencies.

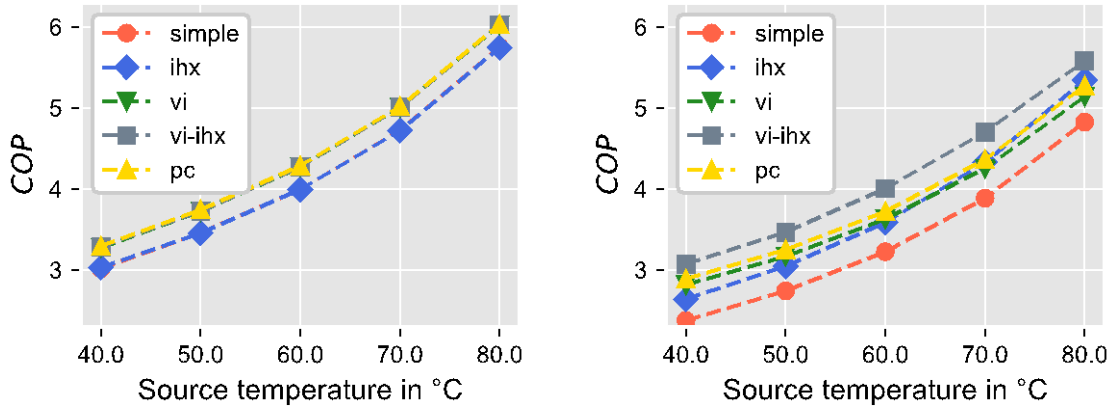

Fig. 5: *COP* results for ammonia (R717 – left) and butane (R600 – right).

The main differences between ammonia and butane result from two aspects: First, ammonia has far higher compressor discharge temperatures (cf. Fig. 4). Second, butane – similar to the other hydrocarbons – has a dewline with a comparably low slope. Thus, the amount of superheating at the compressor outlet and the condenser inlet is relatively low for most operating points and flowsheets. Both effects can improve or reduce the effects mentioned by the individual flowsheets and will be evaluated in the following.

In the ihx flowsheet, the main improvements result from the higher superheating at the compressor inlet and, thus, the higher degree of subcooling at the inlet into the expansion valve. Therefore, the potential can be fully utilized for butane with a low compressor discharge temperature. Furthermore, the improvements in additional heat in the condenser are greater than the additional compressor work due to the higher temperature at the compressor inlet, leading to efficiency improvements. For ammonia with a very high discharge temperature, however, the improvement in additional heat in the condenser is lower compared to the increase in compressor work. Thus, the optimizer does not increase the superheating at the compressor inlet compared to the simple cycle. Hence, the efficiencies are similar.

In the vi flowsheet, the compressor's discharge temperature can be reduced due to the injection of refrigerant vapor at a lower temperature. For ammonia, the throttling losses and the losses due to heat transfer in the condenser can be reduced. Similar effects occur for butane. However, since butane has a low amount of superheating at the compressor outlet (in the simple cycle 6 K for a source temperature of 80 °C), the overall possible improvement is limited. Additionally, the pinch-point temperature is influenced negatively, leading to higher condensation pressures (19.6 bar in the simple cycle compared to 20.5 bar in the vi cycle). In the vi cycle, the pinch-point is located in the superheated region of the sink water. In the simple cycle, the pinch-point is located at the evaporation region of the sink water. Hence, the sink temperature at the pinch-point is higher, leading to higher necessary refrigerant temperatures to satisfy the second law of thermodynamics. This effect negatively influences the overall performance of vi. Hence, vi shows greater improvements for refrigerants with moderate compressor discharge superheating. For lower source temperatures, the amount of discharge superheating at the compressor increases for butane. Therefore, the performance of the vi flowsheets increases also.

The pc flowsheet shows similar effects to the vi cycle. The main difference is the location where both enthalpy flows are mixed. In the vi cycle, the mixing occurs in the compressor leading to a mixing entropy production in the compressor. Simultaneously, the compressor is cooled, leading to lower maximum process temperatures. In the pc flowsheet, the mixing occurs after both compressors. Hence, two effects occur. First,

the maximum process temperature is not influenced compared to the simple cycle since a partial mass flow rate still overcomes the total pressure ratio (cf. Fig. 4). Second, the entropy production due to mixing does not influence the compression process since it occurs after both compressors. Due to the second effect, the efficiencies of pc flowsheet are overall slightly higher compared to the vi flowsheet.

For the vi-ihx flowsheet, the mentioned effects for vi and ihx are combined. However, in the case of ammonia, the ihx does not offer any improvement. Hence, the results of the vi and vi-ihx flowsheets are similar.

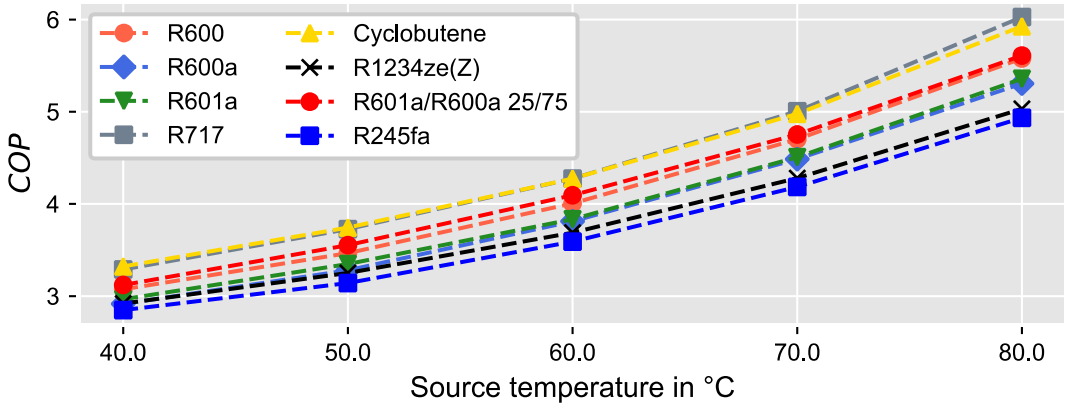

Fig. 6: *COP* for vi-ihx cycle for selected refrigerants.

Finally, Fig. 6 shows the best-performing flowsheet (vi-ihx) results for all refrigerants in dependency on the source inlet temperature. The *COP* increases when the sink inlet temperature increases for all refrigerants. However, the overall refrigerant ranking is not affected by the adjustment of the source temperature. Thus, ammonia and cyclobutene show the highest performances still. Nevertheless, the investigation could only cover some potential refrigerants for applying a steam generation heat pump. Thus, ammonia or cyclobutene are not necessarily the best possible refrigerants. Further research should investigate the possibility and the potential of tailor-made azeotropic mixtures that offers fluid properties for a defined application.

In the following section, the results of the present investigation are discussed.

4. Discussion

The previous section shows the results of the analysis of several refrigerants in five possible cycle configurations for the application in high temperature heat pumps to generate low-pressure steam. Regarding cycle efficiency, ammonia and cyclobutene show the highest values. Additionally, combining an internal heat exchanger and vapor injection in one flowsheet leads to the highest efficiencies for all refrigerants.

Besides the cycle efficiency, however, several further aspects must be addressed when selecting a refrigerant and a flowsheet for an application. One aspect is the long-term chemical stability of refrigerants. In high temperature applications, the refrigerant has to withstand the continuously high temperature compared to conventional heat pump systems (e.g., for space heating). However, long-term stability tests have yet to be conducted for many refrigerants. Thus, the long-term stability is unknown. However, one possible indicator is the molecule structure of a refrigerant. In this regard, double and triple bonds tend to be less chemically stable than regular bonds. Table 1 shows, there a refrigerant molecule includes at least one double or triple bond. Besides the natural refrigerant R717 (ammonia) and the hydrocarbons R600, R600a, and R601a, all investigated refrigerants have at least one double or triple bond. Hence, their chemical stability cannot be guaranteed, and further studies are necessary. Thus, ammonia is preferable to cyclobutane since its long-term stability has been tested widely already.

Ammonia is a toxic and moderately flammable (B2L) refrigerant. Therefore, additional safety measures are necessary, leading to higher costs and a more prolonged designing phase since many regulations must be satisfied. Furthermore, stainless steel is necessary for ammonia, resulting in higher investments. Additionally, processing stainless steel is more challenging and expensive compared to conventional materials for heat pumps, e.g., copper, making the construction part more challenging.

Besides the general fluid properties, ammonia has a critical temperature of 132.4 °C. Since the application of this paper is the generation of low-pressure steam with a water vapor outlet temperature of 120 °C, ammonia operates relatively close to the critical points. In case of higher dynamics or oscillations during the operation,

the critical point might be reached, leading to an unstable operation. Thus, ammonia might not be applicable for the given use case. Ammonia is applicable for lower sink temperatures with a sufficient difference from the critical temperature. Nevertheless, ammonia leads to very high operating pressures due to its high critical pressure of 112.8 bar. For operation closer to the critical temperature, there are limited components available to utilize ammonia's potential. Especially the compressor with its sealings leads to challenges regarding the design of new components.

Additionally, ammonia leads to very high discharge temperatures compared to other refrigerants (cf. Fig. 4), which can negatively affect the lubricant in the compressor. Therefore, oil-free compressor solutions, e.g., turbo compressors, can be possible when handling high temperatures. However, turbo compressors need several compression stages due to the high occurring pressure ratios and the simultaneously only limited pressure ratio a compression stage can overcome. Hence, additional investments are necessary for the system.

Nevertheless, ammonia has been applied in heat pumps for several decades. Thus, the mentioned challenges are well known, and possible solutions have been prepared and proven sufficient for a safe and efficient operation. Also, ammonia has the advantage of high volumetric heat capacities due to its high operating pressure. Due to the high volumetric heat capacities, the components of the heat pumps can be designed smaller, leading to more compact systems. Especially for large-scale heat pumps with heating demands in the range of several megawatts, compact systems are necessary due to the high demand for space. Thus, ammonia shows a high-performance solution for compact heat pump systems with solvable challenges regarding its safe operation.

Regardless of the high performance of ammonia, further research should still be conducted regarding possible alternatives. For example, for steam generation, zeotropic mixtures are not suitable due to the negative effect of the temperature glide. Tailor-made azeotropic mixtures optimized for the individual application, however, might improve the overall cycle performance (efficiency, volumetric heat capacity, maximum process temperature) further, leading to a further reduction in power demand and, thus, carbon emissions.

5. Conclusions

The present investigation analyzes the applicability of heat pumps for the generation of low-pressure steam. For the application, the water enters the heat pump condenser at 80 °C, evaporates at 1.5 bar (approx. 111 °C), and leaves the condenser at 120 °C as superheated vapor. First, a refrigerant selection is conducted to analyze the applicability of heat pumps. We identify 14 refrigerants that are not toxic and have a GWP below 150. Additionally, ammonia is included due to its high performance in existing heat pumps, and R245fa is added as a reference refrigerant. Second, we evaluate the performance of the refrigerants in five flowsheets and analyze the influence of shifting the source temperature from 40 °C to 80 °C.

The results show that ammonia and cyclobutene lead to the highest efficiencies with *COPs* of up to 6. Cyclobutene, however, has a double in its molecule structure and might be less chemically stable than ammonia. Hence, ammonia is to be preferred. Regarding the cycle configuration, a combination of vapor injection and an internal heat exchanger shows the highest efficiencies for all investigated refrigerants. For ammonia, however, the potential is similar to a basic vapor injection cycle since the potential of the internal heat exchanger cannot be utilized due to the high compressor discharge temperatures of ammonia.

Finally, the results are discussed. Due to its toxicity and flammability, additional safety measures are necessary when using ammonia as a refrigerant. Nevertheless, ammonia has been used in heat pumps for decades, showing its potential and solution when dealing with additional safety regulations. Additionally, ammonia leads to compact systems due to its high volumetric efficiency. Hence, ammonia is a performance solution, especially when combined with advanced flowsheets like a two-stage compression. So overall, ammonia is a high-efficiency replacement for conventional refrigerants such as R245fa. However, further research regarding the potential of tailor-made azeotropic mixtures should be conducted since the individual fluid properties can be optimized for generating low-pressure steam, improving the cycle efficiency even further.

Acknowledgements

We gratefully acknowledge the financial support by the German Federal Ministry for Economic Affairs and Climate Action (BMWK), promotional reference 03EN4011.

References

[1] V. Masson-Delmotte *et al., Climate Change 2021: The Physical Science Basis. Contribution of Working Group I to the Sixth Assessment Report of the Intergovernmental Panel on Climate Change*: Cambridge University Press, 2021. [Online]. Available: https://www.ipcc.ch/report/ar6/wg1/

[2] C. Arpagaus, F. Bless, M. Uhlmann, J. Schiffmann, and S. S. Bertsch, "High temperature heat pumps: Market overview, state of the art, research status, refrigerants, and application potentials," *Energy*, vol. 152, pp. 985–1010, 2018, doi: 10.1016/j.energy.2018.03.166.

[3] M. Papapetrou, G. Kosmadakis, A. Cipollina, U. La Commare, and G. Micale, "Industrial waste heat: Estimation of the technically available resource in the EU per industrial sector, temperature level and country," *Applied Thermal Engineering*, vol. 138, pp. 207–216, 2018, doi: 10.1016/j.applthermaleng.2018.04.043.

[4] M. O. McLinden, C. J. Seeton, and A. Pearson, "New refrigerants and system configurations for vapor-compression refrigeration," *Science (New York, N.Y.)*, vol. 370, no. 6518, pp. 791–796, 2020, doi: 10.1126/science.abe3692.

[5] M. O. McLinden, J. S. Brown, R. Brignoli, A. F. Kazakov, and P. A. Domanski, "Limited options for low-global-warming-potential refrigerants," *Nat Commun*, vol. 8, no. 1, p. 14476, 2017, doi: 10.1038/ncomms14476.

[6] J. Navarro-Esbrí, A. Fernández-Moreno, and A. Mota-Babiloni, "Modelling and evaluation of a high-temperature heat pump two-stage cascade with refrigerant mixtures as a fossil fuel boiler alternative for industry decarbonization," *Energy*, vol. 254, p. 124308, 2022, doi: 10.1016/j.energy.2022.124308.

[7] D. Roskosch, V. Venzik, J. Schilling, A. Bardow, and B. Atakan, "Beyond Temperature Glide: The Compressor is Key to Realizing Benefits of Zeotropic Mixtures in Heat Pumps," *Energy Technology*, p. 2000955, 2021, doi: 10.1002/ente.202000955.

[8] M. Jesper, F. Schlosser, F. Pag, T. G. Walmsley, B. Schmitt, and K. Vajen, "Large-scale heat pumps: Uptake and performance modelling of market-available devices," *Renewable and Sustainable Energy Reviews*, vol. 137, p. 110646, 2021, doi: 10.1016/j.rser.2020.110646.

[9] C. Mateu-Royo, C. Arpagaus, A. Mota-Babiloni, J. Navarro-Esbrí, and S. S. Bertsch, "Advanced high temperature heat pump configurations using low GWP refrigerants for industrial waste heat recovery: A comprehensive study," *Energy Conversion and Management*, vol. 229, p. 113752, 2021, doi: 10.1016/j.enconman.2020.113752.

[10] T. Bai, G. Yan, and J. Yu, "Thermodynamic assessment of a condenser outlet split ejector-based high temperature heat pump cycle using various low GWP refrigerants," *Energy*, vol. 179, pp. 850–862, 2019, doi: 10.1016/j.energy.2019.04.191.

[11] D. Roskosch, C. Arpagaus, S. Bertsch, and A. Bardow, "Compressor design vs. refrigerants properties: What is the main influence on compressor efficiency?," *26th International Compressor Engineering Conference at Purdue, July 10-14*, 2022.

[12] Z. Sun *et al.*, "Experimental study on CO2/R32 blends in a water-to-water heat pump system," *Applied Thermal Engineering*, vol. 162, p. 114303, 2019, doi: 10.1016/j.applthermaleng.2019.114303.

[13] M. R. Ally, V. Sharma, and K. Nawaz, "Options for low-global-warming-potential and natural refrigerants part I: Constrains of the shape of the P–T and T–S saturation phase boundaries," *International Journal of Refrigeration*, vol. 106, pp. 144–152, 2019, doi: 10.1016/j.ijrefrig.2019.05.010.

[14] C. Höges, D. Roskosch, J. Brach, C. Vering, V. Venzik, and D. Müller, "Investigation of the Interactions between Refrigerant, Flowsheet, and Compressor in Residential Heat Pumps," *Energy Technol.*, p. 2201295, 2023, doi: 10.1002/ente.202201295.

[15] E. W. Lemmon, I. H. Bell, M. L. Huber, and M. O. McLinden, "NIST Standard Reference Database 23: Reference Fluid Thermodynamic and Transport Properties-REFPROP, Version 10.0, National Institute of Standards and Technology," 2018, doi: 10.18434/T4/1502528.

Appendix

Table 3: Cycle efficiencies (*COP*) of evaluated refrigerants for operating point W80/W120.

Refrigerant	simple cycle	ihx cycle	vi cycle	vi-ihx cycle	pc cycle
R601a (isopentane)	4.43	5.18	4.63	5.36	4.76
R600a (isobutane)	4.41	5.00	4.83	5.31	4.94
R600 (butane)	4.83	5.34	5.14	5.58	5.27
R717 (ammonia)	5.75	5.74	6.02	6.03	6.03
R1224yd(Z)	4.06	4.50	4.35	4.62	4.36
R1233zd(E)	4.40	4.72	4.62	4.88	4.65
R1234ze(Z)	4.50	4.86	4.78	5.03	4.82
R1336mzz(Z)	3.80	4.29	4.04	4.34	4.08
R1336mzz(E)	3.41	4.01	3.82	4.30	3.83
Butene	4.95	5.35	5.35	5.58	5.36
Isobutene	4.41	5.31	5.30	5.56	5.31
Cyclobutene	5.64	5.82	5.86	5.93	5.87
1-Butyne	5.39	5.65	5.72	5.85	5.72
(Z)-But-2-ene	5.27	5.56	5.57	5.73	5.60
(E)-But-2-ene	5.13	5.49	5.48	5.69	5.49
R245fa	4.30	4.75	4.61	4.93	4.63
R601a/R600a 25/75	4.21	5.46	4.68	5.61	4.70